Available online at www.sciencedirect.com
SCIENCE DIRECT®
International Journal of Heat and Fluid Flow 26 (2005) 416–430
International Journal of HEAT AND FLUID FLOW
www.elsevier.com/locate/ijhff

Statistical models for predicting particle dispersion and preferential concentration in turbulent flows

L.I. Zaichik, V.M. Alipchenkov *

Institute for High Temperatures of the Russian Academy of Sciences, Krasnokazarmennaya 17a, Moscow 111116, Russian Federation

Received 10 October 2003; accepted 5 October 2004
Available online 24 November 2004

Abstract

The objective of the paper is to present a statistical approach to modelling dispersion and preferential concentration of inertial particles suspended in the turbulent fluid. This approach departs from kinetic equations for the one-point and two-point probability density functions of particle velocity distributions in turbulent Gaussian fluid flow fields. Preferential concentration of particles in sheared as well as in isotropic turbulent flows is analysed from a unified viewpoint, and an analogy between both phenomena is discussed.

Keywords: Two-phase particle-laden flow; Turbulence; Statistical models; Kinetic equations

1. Introduction

One of the most striking effects of particle interaction with turbulent eddies is an existence of flow regions with preferential concentration. The accumulation (or clustering) effect was established in many numerical and experimental investigations performed in free and bounded turbulent flows (e.g., Fessler et al., 1994; Fukagata et al., 1998; Chen et al., 1998; Rouson and Eaton, 2001; Li et al., 2001; Portela et al., 2001; Cerbelli et al., 2001). In inhomogeneous turbulence, this phenomenon referred to as turbophoresis manifests itself as a tendency of particles to concentrate within certain areas of turbulent flow due to a drift velocity caused by the gradient of the turbulence intensity (Reeks, 1983). However, the accumulation effect occurs also in homogeneous turbulence, when the mean gradient of velocity fluctuations and the conventional turbophoretic force are absent (Squires and Eaton, 1991; Wang and Maxey, 1993; Sundaram and Collins, 1997; Wang et al., 2000; Reade and Collins, 2000; Balkovsky et al., 2001; Février et al., 2001; Hogan and Cuzzi, 2001; Elperin et al., 2002; Sigurgeirsson and Stuart, 2002; Bec, 2003; Zaichik and Alipchenkov, 2003). The clustering of particles in homogeneous turbulence is a fairly sophisticated effect, which remains to be clarified and taken into consideration in existing theories of two-phase turbulent flows. Most of these theories are based on the assumption that particles are independently distributed in space in a perfectly random manner with uniform probability, and thereby preferential concentration is completely ignored. At the same time, the preferential concentration of particles in homogeneous turbulence may play an extremely important role in a number of environmental and industrial processes. For example, the effect of preferential concentration can lead to substantial increase in both particle settling velocities and coalescence rates.

The purpose of this paper is to advance a rational approach to modelling dispersion and preferential concentration of inertial particles immersed in turbulent fluid flow. This approach is based on kinetic equations for

* Corresponding author. Fax: +7 095 362 55 90.
E-mail address: leonid.zaichik@mtu-net.ru (V.M. Alipchenkov).

0142-727X/$ - see front matter © 2004 Elsevier Inc. All rights reserved.
doi:10.1016/j.ijheatfluidflow.2004.10.001

Nomenclature

A_1, A_2 constants
$B_{\mathrm{L}ij}$ Lagrangian correlation function
C, C_1, $C_{0\infty}$ constants
D_{ij}, D^r_{ij} one-point and two-point diffusivity tensors of a noninertial admixture
$D_{p\mathrm{ij}}$, D^r_{pij} particle and particle-pair diffusivity tensors
$\mathbf{F}$ external force (e.g., gravity) acceleration vector
f_u, f_{u1}, g_u, l_u particle response coefficients
f_r, g_r, f_{r1}, l_r particle-pair response coefficients
H Heaviside function
L turbulence spatial macroscale
l_+ dimensionless Prandtl–Nikuradse mixing length
N particle-pair density
P_v, P_w one-point and two-point PDF
p_v, p_w one-point and two-point particle probability densities
R channel half-width or pipe radius
$\mathbf{R}_p$ particle position vector
R_+ dimensionless channel half-width or pipe radius, Ru_*/ν
$\mathbf{r}$ separation vector
r separation distance, $|\mathbf{r}|$
$\mathbf{r}_p$ separation vector, $\mathbf{R}_{p2} - \mathbf{R}_{p1}$
$\bar{r}$ dimensionless separation distance, $\bar{r} = r/\eta$
Re_λ Taylor-scale Reynolds number, $(15u'^4/\varepsilon\nu)^{1/2}$
S_{ij}, S_{pij} second-order Eulerian fluid and particle velocity structure functions
$\overline{S}_{ij}$, $\overline{S}_{pij}$ dimensionless fluid and particle structure functions, S_{ij}/u_k^2, S_{pij}/u_k^2
S_{ijk}, S_{pijk} third-order Eulerian fluid and particle velocity structure functions
St Stokes number, τ_p/τ_k
T_{L}, $T_{\mathrm{L}r}$ one-point and two-point Lagrangian integral timescales
$T_{\mathrm{L}+}$ dimensionless Lagrangian integral timescale, $T_{\mathrm{L}}u_*^2/\nu$
$\overline{T}_{\mathrm{L}r}$ dimensionless two-point timescale, $T_{\mathrm{L}r}/\tau_k$
t time
U_i, u_i, u'_i mean, total, and fluctuating fluid velocities
u_k Kolmogorov velocity microscale, $(\nu\varepsilon)^{1/4}$
u_* wall friction velocity
u'^2 fluid velocity variance
$\langle u'^2_{y+}\rangle$ dimensionless fluid wall-normal stress, $\langle u'^2_y\rangle/u_*^2$
u'_{y+} fluid wall-normal fluctuating velocity, $\langle u'^2_{y+}\rangle^{1/2}$
$\langle u'_i u'_j\rangle$ fluid Reynolds stresses
V_i, v_i, v'_i mean, total, and fluctuating particle velocities
$\mathbf{v}_p$ velocity vector of a particle
$\langle v'^2_{y+}\rangle$ dimensionless particulate wall-normal stress, $\langle v'^2_y\rangle/u_*^2$
v'_{y+} particle wall-normal fluctuating velocity, $\langle v'^2_{y+}\rangle^{1/2}$
$\langle v'_i v'_j\rangle$ particulate kinetic stresses
W_i, w_i, w'_i mean, total, and fluctuating relative velocities
$\mathbf{w}_p$ relative velocity between two particles, $\mathbf{v}_{p2} - \mathbf{v}_{p1}$
$\mathbf{x}$ coordinate vector
y wall-normal coordinate
y_+ dimensionless wall-normal coordinate, yu_*/ν
$\bar{y}$ dimensionless wall-normal coordinate, y/R

Greeks

α exponent
β collision kernel
Γ radial distribution function, $N/N(r=\infty)$
ΔU_i, Δu_i, $\Delta u'_i$ mean, total, and fluctuating fluid velocity increments
δ delta-function or functional derivative
δ_{ij} Kronecker symbol
ε energy dissipation rate
η Kolmogorov length microscale, $(\nu^3/\varepsilon)^{1/4}$
κ Prandtl–Karman constant
ν fluid kinematic viscosity
σ collision sphere radius
τ time increment
τ_k Kolmogorov time microscale, $(\nu/\varepsilon)^{1/2}$
τ_p particle response time
τ_+ dimensionless particle response time, $\tau_p u_*^2/\nu$
Φ particle averaged volume fraction
φ Green function
Ψ_{L}, $\Psi_{\mathrm{L}r}$ one-point and two-point autocorrelation functions

the one-point and two-point probability density functions (PDF) of particle velocity distributions in turbulent Gaussian fluid flow fields. The PDF method is a powerful tool routinely used in continuum mechanics for developing hydrodynamic models. In particular, introducing the PDF permits to proceed from the dynamic stochastic description of separate particles to the statistical modelling of the behaviour of a particle ensemble immersed in turbulent flow. The PDF modelling approach starts from the Lagrangian equations for individual particles, and a kinetic equation is derived that governs the PDF of particle position, velocity, temperature, size, and other variables of interest (e.g., Derevich and Zaichik, 1988; Reeks, 1991; Simonin,

1996; Swailes and Darbyshire, 1997; Hyland et al., 1999; Pozorrski and Minier, 1999; Zaichik, 1999; Derevich, 2000; Pandya and Mashayek, 2003). From the kinetic equation, one can gain a set of continuum conservation equations for the statistical moments of the PDF. These conservation equations govern the averaged properties of the dispersed phase in the framework of the Eulerian modelling formalism.

The present paper extends the one-point and two-point kinetic PDF models (Zaichik, 1999; Zaichik and Alipchenkov, 2003) to include the transport effect in the approximations of Lagrangian velocity correlations. The particle volume fraction is kept small enough so that the two-phase system is quite good within the dilute limit, the particles do not influence the carrier fluid flow, and turbulence modulation may be neglected. The accumulation of inertial particles in inhomogeneous sheared and homogeneous isotropic turbulent flows will be analysed from a unified viewpoint, and an analogy between both phenomena will be revealed. In the paper we focus on the transport of monodisperse particles immersed in isothermal turbulent flow, and hence we manipulate with the PDF in respect to particle position and velocity. To extend these models to polydisperse particle system in non-isothermal turbulent flow, one has to handle with the probability density of particle size and temperature as well, but this is beyond the scope of the paper.

2. One-point PDF model

Let us firstly consider the one-point PDF model. This model is applicable to predicting one-particle statistics and single-particle dispersion in inhomogeneous sheared turbulence.

The motion of a small heavy particle in a turbulent fluid flow is governed by the following equations:

$$\frac{\mathrm{d}\mathbf{R}_p}{\mathrm{d}t} = \mathbf{v}_p, \quad \frac{\mathrm{d}\mathbf{v}_p}{\mathrm{d}t} = \frac{\mathbf{u}(\mathbf{R}_p,t) - \mathbf{v}_p}{\tau_p} + \mathbf{F}, \tag{1}$$

where $\mathbf{u}(\mathbf{R}_p,t)$ symbolizes the local instantaneous velocity of the carrier fluid at a point $\mathbf{x} = \mathbf{R}_p(t)$.

The one-point PDF of particle velocity is introduced by

$$P_v = \langle p_v \rangle = \langle \delta\big(\mathbf{x} - \mathbf{R}_p(t)\big)\delta(\mathbf{v} - \mathbf{v}_p(t))\rangle, \tag{2}$$

where $\langle\rangle$ denotes an averaging procedure over an ensemble of samples of a random fluid velocity field, and $P_v(\mathbf{x},\mathbf{v},t)$ stands for the probability of finding a particle at a point $\mathbf{x}$, with a velocity $\mathbf{v}$, at time t. Differentiating (2) with respect to time, decomposing the fluid velocity field into the sum of averaged and fluctuating components ($\mathbf{u} = \mathbf{U} + \mathbf{u}'$), and accounting for (1), we gain the following transport equation for the PDF:

$$\frac{\partial P_v}{\partial t} + v_k\frac{\partial P_v}{\partial x_k} + \frac{\partial}{\partial v_k}\left[\left(\frac{U_k - v_k}{\tau_p} + F_k\right)P_v\right] = -\frac{1}{\tau_p}\frac{\langle u'_k p_v\rangle}{\partial v_k}. \tag{3}$$

The left-hand side of Eq. (3) describes evolution in time and convection in phase space $(\mathbf{x},\mathbf{v})$, whereas the term on the right side characterizes the interaction between particles and fluid turbulent eddies. Equation (7) becomes a closed one as soon as a closure model for $\langle u'_k p_v\rangle$ is provided. With this in mind, we will model the fluid velocity by a Gaussian random process with known one-point correlation moments. By this means, using the Furutsu–Donsker–Novikov formula for Gaussian random functions (Frisch, 1995), we derive

$$\langle u'_i p_v\rangle = \int\int \langle u'_i(\mathbf{x},t)u'_k(\mathbf{x}_1,t_1)\rangle\left\langle\frac{\delta p_v(\mathbf{x},t)}{\delta u_k(\mathbf{x}_1,t_1)\mathrm{d}\mathbf{x}_1\,\mathrm{d}t_1}\right\rangle\mathrm{d}\mathbf{x}_1\,\mathrm{d}t_1,$$

$$\left\langle\frac{\delta p_v(\mathbf{x},t)}{\delta u_k(\mathbf{x}_1,t_1)\mathrm{d}\mathbf{x}_1\,\mathrm{d}t_1}\right\rangle = -\frac{\partial}{\partial x_j}\left\langle p_v(\mathbf{x},t)\frac{\delta R_{pj}(t)}{\delta u_k(\mathbf{x}_1,t_1)\mathrm{d}\mathbf{x}_1\,\mathrm{d}t_1}\right\rangle - \frac{\partial}{\partial v_j}\left\langle p_v(\mathbf{x},t)\frac{\delta v_{pj}(t)}{\delta u_k(\mathbf{x}_1,t_1)\,\mathrm{d}\mathbf{x}_1\,\mathrm{d}t_1}\right\rangle. \tag{4}$$

For obtaining the functional derivatives in (4) we represent the solutions of Eq. (1) in terms of integrals taken along a particle trajectory

$$\mathbf{R}_p(t) = \int_0^t \mathbf{v}_p(t_1)\,\mathrm{d}t_1,$$

$$\mathbf{v}_p(t) = \int_0^t \varphi(t-t_1)\big[\mathbf{u}(\mathbf{R}_p(t_1),t_1) + \tau_p\mathbf{F}\big]\mathrm{d}t_1,$$

$$\varphi(t) = \frac{1}{\tau_p}\exp\left(-\frac{\mathrm{t}}{\tau_\mathrm{p}}\right), \tag{5}$$

where $\varphi(t)$ symbolizes the Green function.

Applying the functional differentiation operator to (5), we obtain a set of integral equations for determining the functional derivatives:

$$\frac{\delta R_{pi}(t)}{\delta u_j(\mathbf{r}_1,t_1)\mathrm{d}\mathbf{x}_1\,\mathrm{d}t_1} = \delta_{ij}\delta(\mathbf{x}_1 - \mathbf{R}_p(t_1))\int_{t_1}^t \varphi(t-t_2)\mathrm{d}t_2 + \int_{t_1}^t\int_{t_2}^t \varphi(t-t_3)\mathrm{d}t_3\frac{\partial u_i(\mathbf{R}_p(t_2),t_2)}{\partial x_n} \times \frac{\delta R_{pn}(t_2)}{\delta u_j(\mathbf{x}_1,t_1)\mathrm{d}\mathbf{x}_1\,\mathrm{d}t_1}\mathrm{d}t_2, \tag{6}$$

$$\frac{\delta v_{pi}(t)}{\delta u_j(\mathbf{x}_1,t_1)\mathrm{d}\mathbf{x}_1\,\mathrm{d}t_1} = \delta_{ij}\delta(\mathbf{x}_1 - \mathbf{R}_p(t_1))\varphi(t-t_1)H(t-t_1) + \int_{t_1}^t \varphi(t-t_2)\frac{\partial u_i(\mathbf{R}_p(t_2),t_2)}{\partial x_n} \times \frac{\delta R_{pn}(\tau_2)}{\delta u_j(\mathbf{x}_1,t_1)\mathrm{d}\mathbf{x}_1\,\mathrm{d}t_1}\mathrm{d}t_2,$$

where $H(x)$ is the Heaviside function: $H(x<0) = 0$, $H(x>0) = 1$.

To solve (6) we use an iteration procedure employed previously in Zaichik (1997, 1999). Then, averaging the functional derivatives over the particle probability density p_v and accounting for a single term containing the fluid velocity gradient, we rearrange (4) in the form

$$\langle u_i' p_v\rangle = -\int_{t_1}^{t}\langle u_i'(\mathbf{x},t)u_j'(\mathbf{R}_p(t_1),t_1)\rangle\int_{t_1}^{t}\varphi(t-t_2)\,\mathrm{d}t_2\,\mathrm{d}t_1\frac{\partial P_v}{\partial x_j} - \int_{t_1}^{t}\langle u_i'(\mathbf{x},t)u_k'(\mathbf{R}_p(t_1),t_1)\rangle\left[\delta_{jk}\varphi(t-t_1) + \frac{\partial U_j}{\partial x_k}\int_{t_1}^{t}\varphi(t-t_2)\int_{t_1}^{t_2}\varphi(t_2-t_3)\,\mathrm{d}t_3\,\mathrm{d}t_2\right]\mathrm{d}t_1\frac{\partial P_v}{\partial v_j}. \tag{7}$$

With a view to determine the trajectory integrals in (7), we define the Lagrangian one-point correlation function of fluid velocities by the following approximation:

$$\begin{aligned} B_{\mathrm{L}ij}(\mathbf{x},t,\tau) &= \langle u_i'(\mathbf{x},t)u_j'(\mathbf{R}_p(t-\tau),t-\tau)\mid \mathbf{R}_p(t)=\mathbf{x}\rangle \\ &= \langle u_i'(\mathbf{x},t-\tau/2)u_j'(\mathbf{x},t-\tau/2)\rangle\,\Psi_{\mathrm{L}}(\tau) \\ &= \left[\langle u_i'(\mathbf{x},t)u_j'(\mathbf{x},t)\rangle - \frac{\tau}{2}\frac{D\langle u_i'(\mathbf{x},t)u_j'(\mathbf{x},t)\rangle}{Dt}\right]\Psi_{\mathrm{L}}(\tau), \end{aligned} \tag{8}$$

$$\frac{D\langle u_i'u_j'\rangle}{Dt} = \left(\frac{\partial\langle u_i'u_j'\rangle}{\partial t} + U_k\frac{\partial\langle u_i'u_j'\rangle}{\partial x_k} + \frac{\partial\langle u_i'u_j'u_k'\rangle}{\partial x_k}\right).$$

Here $\Psi_{\mathrm{L}}(\tau)$ designates the autocorrelation function that is specified by the Lagrangian integral timescale $T_{\mathrm{L}} = \int_0^\infty \Psi_{\mathrm{L}}(\tau)\,\mathrm{d}\tau$. Eq. (8) contains an additional term in parentheses as compared to the conventional approximation $B_{\mathrm{L}ij}(\mathbf{x},t,\tau) = \langle u_i'(\mathbf{x},t)u_j'(\mathbf{x},t)\rangle\Psi_{\mathrm{L}}(\tau)$. This term, first introduced by Derevich (2000), takes into consideration the transport effect due to turbulence unsteadiness as well as the convective and diffusive transfer of fluid velocity fluctuations along a particle trajectory. It is clear that, in stationary homogeneous turbulence, the "transport term" in (8) is absent. In the following, we assume that the fluid velocity correlations viewed by the particles are the same as those along the fluid-element trajectories. Obviously this assumption is strictly valid in the zero-inertia limit and fails for high-inertia particles (e.g., Reeks, 1977; Wang and Stock, 1993). It should be mentioned that the identification of $\Psi_{\mathrm{L}}(\tau)$ with the standard fluid Lagrangian autocorrelation function is not a crucial point in this approach, because it is possible to generalize the model using any autocorrelation function that accounts for the inertia and crossing trajectory effects.

By means of (8), we can obtain the following expression for the correlation between the fluid fluctuating velocity and the particle probability density:

$$\langle u_i' p_v\rangle = -\langle u_i'u_j'\rangle\left(f_u\frac{\partial P_v}{\partial v_j} + \tau_p g_u\frac{\partial P_v}{\partial x_j}\right) + \frac{\tau_p f_{u1}}{2}\frac{D\langle u_i'u_j'\rangle}{Dt}\frac{\partial P_v}{\partial v_j} - \tau_p l_u\langle u_i'u_k'\rangle\frac{\partial U_j}{\partial x_k}\frac{\partial P_v}{\partial v_j}, \tag{9}$$

$$\begin{aligned} f_u &= \frac{1}{\tau_p}\int_0^\infty \Psi_{\mathrm{L}}(\tau)\exp\left(-\frac{\tau}{\tau_p}\right)\mathrm{d}\tau, \\ g_u &= \frac{T_{\mathrm{L}}}{\tau_p} - f_u, \\ f_{u1} &= \frac{1}{\tau_p^2}\int_0^\infty \Psi_{\mathrm{L}}(\tau)\tau\exp\left(-\frac{\tau}{\tau_p}\right)\mathrm{d}\tau, \quad l_u = g_u - f_{u1}. \end{aligned} \tag{10}$$

The coefficients f_u, g_u, f_{u1}, and l_u measure a response of a particle to velocity fluctuations of the fluid. Eq. (9) along with (10) holds for values of time that are long compared with the Lagrangian integral timescale. If the autocorrelation function is described by the frequently used exponential approximation $\Psi_{\mathrm{L}} = \exp(-\tau/T_{\mathrm{L}})$, the response coefficients take the form

$$\begin{aligned} f_u &= \frac{T_{\mathrm{L}}}{\tau_p + T_{\mathrm{L}}}, \quad g_u = \frac{T_{\mathrm{L}}^2}{\tau_p(\tau_p + T_{\mathrm{L}})}, \\ f_{u1} &= \frac{T_{\mathrm{L}}^2}{(\tau_p + T_{\mathrm{L}})^2}, \quad l_u = \frac{T_{\mathrm{L}}^3}{\tau_p(\tau_p + T_{\mathrm{L}})^2}. \end{aligned} \tag{11}$$

Substituting (9) into (3) yields the following transport equation for the one-point (one-particle) PDF of particle velocity distribution in turbulent sheared flow:

$$\begin{aligned} &\frac{\partial P_v}{\partial t} + v_k\frac{\partial P_v}{\partial x_k} + \frac{\partial}{\partial v_k}\left[\left(\frac{U_k - v_k}{\tau_p} + F_k\right)P_v\right] + \frac{f_{u1}}{2}\frac{D\langle u_i'u_k'\rangle}{Dt}\frac{\partial^2 P_v}{\partial v_i\partial v_k} \\ &\quad = \langle u_i'u_k'\rangle\left(\frac{f_u}{\tau_p}\frac{\partial^2 P_v}{\partial v_i\partial v_k} + g_u\frac{\partial^2 P_v}{\partial x_i\partial v_k} + l_u\frac{\partial U_n}{\partial x_k}\frac{\partial^2 P_v}{\partial v_i\partial v_n}\right). \end{aligned} \tag{12}$$

Kinetic Eq. (12) describes the convective transport of the PDF in phase space $(\mathbf{x},\mathbf{v})$ and the diffusive transfer caused by the eddy–particle interaction. Modelling fluid turbulence by means of a Gaussian process with known Lagrangian correlations enables the eddy–particle interaction to be expressed explicitly in the form of the second-order differential operator. When the terms containing the coefficients f_{u1} and l_u are neglected, (12) reduces to the kinetic equation obtained by Derevich and Zaichik (1988) and Reeks (1991) for a homogeneous unsheared flow field. The terms containing the coefficients f_{u1} and l_u take into consideration, respectively, the effect of turbulence unsteadiness and inhomogeneity and the impact of mean fluid velocity gradients. It should be mentioned that the kinetic equations presented in Zaichik (1997, 1999) include the terms of the second-order degree in mean velocity gradients. However, the

influence of these second-order degree terms on particle dispersion is of minor importance, and therefore these are not taken into account in the present paper.

Eq. (12) generates a set of governing continuum equations describing the conservation of mass, momentum, and particulate stresses as the appropriate statistical one-point moments of the one-particle velocity PDF

$$\frac{\partial \Phi}{\partial t}+\frac{\partial \Phi V_k}{\partial x_k}=0, \tag{13}$$

$$\frac{\partial V_i}{\partial t}+V_k\frac{\partial V_i}{\partial x_k}=-\frac{\partial\langle v_i'v_k'\rangle}{\partial x_k}+\frac{U_i-V_i}{\tau_p}+F_i -\frac{D_{pik}}{\tau_p}\frac{\partial \ln \Phi}{\partial x_k}, \tag{14}$$

$$\begin{aligned}&\frac{\partial\langle v_i'v_j'\rangle}{\partial t}+V_k\frac{\partial\langle v_i'v_j'\rangle}{\partial x_k}+\frac{1}{\Phi}\frac{\partial \Phi\langle v_i'v_j'v_k'\rangle}{\partial x_k}+f_{u1}\frac{D\langle u_i'u_j'\rangle}{Dt}\\ &\quad=-\left(\langle v_i'v_k'\rangle+g_u\langle u_i'u_k'\rangle\right)\frac{\partial V_j}{\partial x_k}\\ &\qquad-\left(\langle v_j'v_k'\rangle+g_u\langle u_j'u_k'\rangle\right)\frac{\partial V_i}{\partial x_k}\\ &\qquad+l_u\left(\langle u_i'u_k'\rangle\frac{\partial U_j}{\partial x_k}+\langle u_j'u_k'\rangle\frac{\partial U_i}{\partial x_k}\right)\\ &\qquad+\frac{2}{\tau_p}\left(f_u\langle u_i'u_j'\rangle-\langle v_i'v_j'\rangle\right),\end{aligned} \tag{15}$$

where

$$\Phi=\int P_v\,\mathrm{d}\mathbf{v},\quad V_i=\frac{1}{\Phi}\int v_iP_v\,\mathrm{d}\mathbf{v},$$

$$\langle v_i'v_j'\rangle=\frac{1}{\Phi}\int (v_i-V_i)(v_j-V_j)P_v\,\mathrm{d}\mathbf{v},$$

$$\langle v_i'v_j'v_k'\rangle=\frac{1}{\Phi}\int (v_i-V_i)(v_j-V_j)(v_k-V_k)P_k d\mathbf{v},$$

$$D_{pij}=\tau_p\left(\langle v_i'v_j'\rangle+g_u\langle u_i'u_j'\rangle\right).$$

Here Φ and V_i are the particle averaged volume fraction and velocity, $\langle v_i'v_j'\rangle$ are the turbulent particulate stresses induced by the entrainment of particles into the fluctuating motion of the carrier phase, and D_{pij} is the particle diffusivity tensor.

To close the infinite equation set stemming from (12) at the second-order closure level of (13)–(15), we invoke a gradient algebraic approximation for the triple particle fluctuating velocity correlations. This approximation follows from the corresponding differential equation for the third moments by neglecting time evolution, convection, and generation due to mean velocity gradients as well as by using a quasi-Gaussian approximation for the fourth-rank correlations (Simonin, 1991; Zaichik and Vinberg, 1991)

$$\langle v_i'v_j'v_k'\rangle=-\frac{1}{3}\left(D_{pin}\frac{\partial\langle v_j'v_k'\rangle}{\partial x_n}+D_{pjn}\frac{\partial\langle v_i'v_k'\rangle}{\partial x_n}+D_{pkn}\frac{\partial\langle v_i'v_j'\rangle}{\partial x_n}\right). \tag{16}$$

In should be noted that the closure approximation (16) was also derived by Swailes et al. (1998) and Derevich (2000) by means of the Chapman–Enskog perturbation procedure for solving the kinetic PDF equation.

In the zero-inertia limit ($\tau_p\to 0$), it is follows from (15) that the turbulent stresses in the dispersed and fluid phases are coincident

$$\lim_{\tau_p\to 0}\langle v_i'v_j'\rangle=\langle u_i'u_j'\rangle, \tag{17}$$

and the diffusivity tensor of a noninertial admixture is determined by the expression

$$D_{ij}=\lim_{\tau_p\to 0}D_{pij}=T_{\mathrm{L}}\langle u_i'u_j'\rangle. \tag{18}$$

Substitution of (17) and (18) into (16) rearranges the third-order one-point moments of fluid fluctuating velocities in the form

$$\begin{aligned}\langle u_i'u_j'u_k'\rangle&=\lim_{\tau_p\to 0}\langle v_i'v_j'v_k'\rangle\\ &=-\frac{T_{\mathrm{L}}}{3}\left(\langle u_i'u_n'\rangle\frac{\partial\langle u_j'u_k'\rangle}{\partial x_n}+\langle u_j'u_n'\rangle\frac{\partial\langle u_i'u_k'\rangle}{\partial x_n}\right.\\ &\quad\left.+\langle u_k'u_n'\rangle\frac{\partial\langle u_i'u_j'\rangle}{\partial x_n}\right),\end{aligned} \tag{19}$$

which corresponds to the approximation that was first proposed by Hanjalić and Launder (1972).

As was shown in Swailes et al. (1998), Zaichik (1999), Derevich (2000), and other works, the PDF modelling method is more valid for higher particle inertia when the particle velocity distribution is nearly Gaussian. Nonetheless, it provides a correct limit for fine particles. In particular, the present model leads to the familiar relationships for the diffusivity tensor (18) and the third-order fluctuating velocity moments (19) of fluid particles. Moreover, even though the accuracy of the closure approximation (16) decreases with reducing particle inertia, Eq. (15) suggests that the contribution of diffusion transfer to the balance of the particulate stresses tends to decrease as well. Thus, we hope that the second-order closure model (13)–(16) will give quite good results over the entire range of particle inertia.

3. Particle dispersion in channel turbulent flow

The one-point model is employed to predicting preferential concentration of particles in vertical, fully developed, turbulent flows inside flat and round channels. We consider the case of bouncing particles when the deposition of particles on the walls does not take place. In this situation the particle velocity towards the wall is absent, and hence the only cause responsible for the nonuniformity of

particle distribution across the channel section is the turbulent migration (turbophoresis) due to the gradient of transverse velocity fluctuations. By this means, the equation set governing particle dispersion consists of the balance equations for momentum and fluctuating energy in the wall-normal direction. In accordance with (14)–(16) and (19), these balance equations are written as

$$\Phi\frac{\mathrm{d}\langle v_{y+}'^2\rangle}{\mathrm{d}y_+}+\left(\langle v_{y+}'^2\rangle+g_u\langle u_{y+}'^2\rangle\right)\frac{\mathrm{d}\Phi}{\mathrm{d}y_+}=0, \tag{20}$$

$$\begin{aligned}&\tau_+^2\left\{\frac{\mathrm{d}}{\mathrm{d}y_+}\left[(R_+-y_+)^\alpha\Phi\left(\langle v_{y+}'^2\rangle+g_u\langle u_{y+}'^2\rangle\right)\frac{\mathrm{d}\langle v_{y+}'^2\rangle}{\mathrm{d}y_+}\right]\right.\\&\quad\left.-2\alpha\Phi\left(\langle v_{y+}'^2\rangle+g_u\langle u_{y+}'^2\rangle\right)\frac{\mathrm{d}\langle v_{y+}'^2\rangle}{\mathrm{d}y_+}\right\}\\&\quad+\tau_+f_{u1}\Phi\left\{\frac{\mathrm{d}}{\mathrm{d}y_+}\left[(R_+-y_+)^\alpha T_{\mathrm{L}+}\langle u_{y+}'^2\rangle\frac{\mathrm{d}\langle u_{y+}'^2\rangle}{\mathrm{d}y_+}\right]\right.\\&\quad\left.-2\alpha T_{\mathrm{L}+}\langle u_{y+}'^2\rangle\frac{\mathrm{d}\langle u_{y+}'^2\rangle}{\mathrm{d}y_+}\right\}\\&\quad+2(R_+-y_+)^\alpha\Phi\left(f_u\langle u_{y+}'^2\rangle-\langle v_{y+}'^2\rangle\right)=0.\end{aligned} \tag{21}$$

Eqs. (20) and (21) are represented in a non-dimensional form based on "wall units". The exponent α is equal, respectively, to zero for a flat channel and unity for a round pipe. Momentum equation (20) expresses the balance between the turbophoretic and diffusion forces acting on particles in the wall-normal direction. Obviously, if the gravitational or other body force effect is of importance (e.g., in horizontal channel flow), this body force should be incorporated into the momentum balance equation (20). Eq. (21) includes the terms describing the diffusion transfer of transverse particle fluctuating velocities and the exchange of fluctuations between the particulate and fluid phases. As was mentioned above, the contribution of the diffusion transfer of velocity fluctuations to Eq. (21) decreases with particle inertia. Eqs. (20) and (21), exclusive the second term in (21) which stems from the "transport term" in the Lagrangian velocity correlation (8), are similar to those used by Sergeev et al. (2002) to analyse the near-wall behaviour of high-inertia particles in the channel flow. However, because of providing the zero-inertia limit and reducing the contribution of diffusion transfer as the particle response time decreases, we can believe that Eqs. (20) and (21) hold over the entire range of particle inertia, and not just in the case of high-inertia particles.

To formulate the boundary conditions, we assume the particles to bounce elastically on the walls. Then the boundary conditions for Eqs. (20) and (21) are given by

$$\begin{aligned}&\frac{\mathrm{d}\langle v_{y+}'^2\rangle}{\mathrm{d}y_+}=0\quad\text{for}\quad y_+=0;\quad\frac{\mathrm{d}\langle v_{y+}'^2\rangle}{\mathrm{d}y_+}=0,\\&\Phi=1\quad\text{for}\quad y_+=R_+.\end{aligned} \tag{22}$$

The response coefficients that enter into (20) and (21) are determined by (11), where the Lagrangian timescale is given either by the relation proposed in Kallio and Reeks (1989)

$$T_{\mathrm{L}+}=\begin{cases}10 & \text{for } y_+\geqslant 5\\ 7.122+0.5731y_+-0.00129y_+^2 & \text{for } 5<y_+\leqslant 200\end{cases} \tag{23}$$

or by the relation based on the Prandtl–Nikuradse mixing length (Zaichik et al., 1995)

$$\begin{aligned}&T_{\mathrm{L}+}=(100+l_+^2)^{1/2},\\&l_+=\kappa y_+(1-1.1\bar{y}+0.6\bar{y}^2-0.15\bar{y}^3),\quad\kappa=0.4.\end{aligned} \tag{24}$$

Eqs. (20) and (21) are solved numerically using the tridiagonal-matrix algorithm along with an iteration procedure. To avoid a numerical instability, boundary conditions (22) should be approximated with an accuracy of the no-less-than second order. The results obtained by this means are compared with LES by Fukagata et al. (1998) in a flat channel as well as with DNS data by Portela et al. (2001) in a round pipe. However, first we present solutions to this problem in the zero-inertia and high-inertia limits. In the zero-inertia limit ($\tau_+=0$), it follows from (21) and (22):

$$\langle v_{y+}'^2\rangle=\langle u_{y+}'^2\rangle,\quad\Phi=1. \tag{25}$$

According to (25), non-inertial particles are entirely entrained into the turbulent motion of the carrier fluid, and consequently they are uniformly distributed across the channel section.

In the asymptotic case of particles with much larger response time as compared to the Lagrangian integral timescale ($\tau_+\gg T_{\mathrm{L}+}$), the problem being considered possesses a simple solution. Owing to intensive transverse diffusion transport of velocity fluctuations, the distributions of fluctuating velocity and concentration of high-inertia particles in the channel cross-section are nearly uniform:

$$\langle v_{y+}'^2\rangle=\frac{2^\alpha}{R_+^{1+\alpha}\tau_+}\int_0^{R_+}(R_+-y_+)^\alpha T_{\mathrm{L}+}\langle u_{y+}'^2\rangle\mathrm{d}y_+,\quad\Phi=1. \tag{26}$$

Fig. 1(a) represents the predicted and simulated profiles of the r.m.s. wall-normal fluctuating velocities of the fluid and dispersed phases across the section of a flat channel for $R_+=180$. Curve 1 corresponds to the fluid, notations 2 and 4 relate to middle-inertia particles, and symbols 3 and 5 relate to high-inertia particles. It is clear that both the predictions and the simulations exhibit greater differences in the particle fluctuating velocity relative to the fluid one with increasing particle inertia. The wall-normal fluctuating velocity of high-inertia particles is nearly homogeneous and significantly less than that of the fluid in the turbulent core of the flow. By contrast,

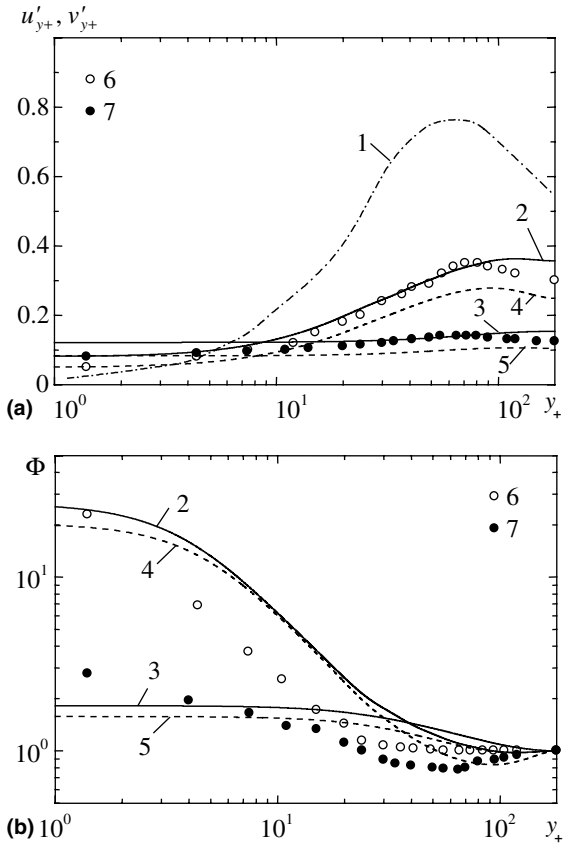

Fig. 1. Profiles of fluctuating velocities (a) and particle concentration (b) in a flat channel: (1) u'_{y+}; (2)–(7) v'_{y+}; (2) and (3) predictions by using (23); (4) and (5) predictions by using (24); (1), (6) and (7) LES by Fukagata et al. (1998); (2), (4) and (6) $\tau_+ = 117$; (3), (5) and (7) $\tau_+ = 810$.

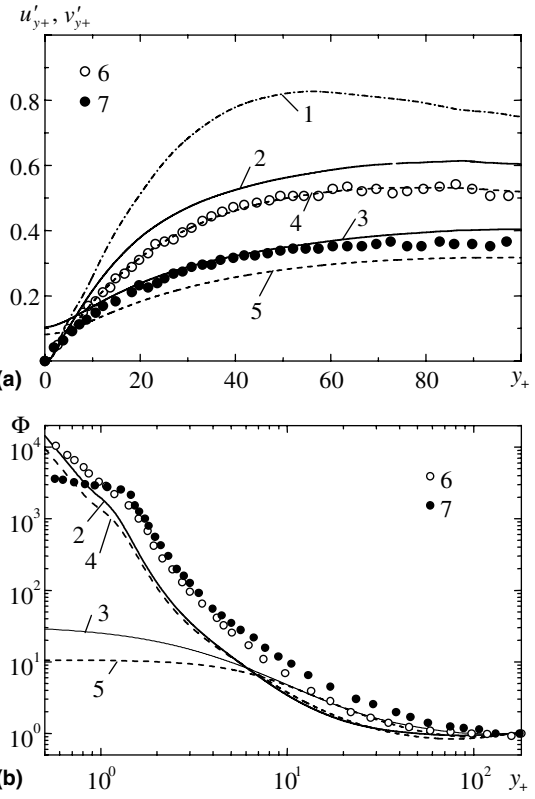

Fig. 2. Profiles of fluctuating velocities (a) and particle concentration (b) in a round pipe: (1) u'_{y+}; (2)–(7) v'_{y+}; (2) and (3) predictions by using (23); (4) and (5) predictions by using (24); (1), (6) and (7) DNS by Portela et al. (2001); (2), (4) and (6) $\tau_+ = 25$; (3), (5) and (7) $\tau_+ = 100$.

in the viscous sub-layer, the particle fluctuating velocity exceeds the fluid one. This effect is attributable to the diffusion transport of turbulent fluctuations from the turbulent core towards the wall. Owing to turbulent diffusion, the fluctuating velocity of relatively inertial particles has a non-zero value on the wall, despite the fact that the corresponding fluid fluctuating velocity is equal to zero. The behaviour of wall-normal velocity fluctuations is crucial to explain a tendency of particles with a certain range of inertia to accumulate in the viscous sub-layer near the wall (Fig. 1(b)). Due to a gradient in the intensity of wall-normal velocity fluctuations, the particles will tend to migrate to regions of lower turbulence energy. In other words, the particles are pushed by the gradient of turbulence intensity towards the wall and "trapped" in the viscous wall region. As is seen from Fig. 1(a), the particle fluctuating velocity profiles predicted on the basis of (20)–(23) are in good agreement with the LES data of Fukagata et al. (1998). Fig. 1(b) demonstrates a qualitative agreement between the predicted and simulated distributions of particle concentration.

In Fig. 2 we compare the predicted and simulated profiles of wall-normal particle fluctuating velocity and concentration in a round pipe for $R_+ = 180$. As can be observed, the predictions obtained with the use of (23) or (24) for the Lagrangian timescale, like the flat channel flow, are quite close. It is also seen from Fig. 2(b) that the particle concentration of low-inertia particles has a singularity at $y = 0$. On the whole, the prediction results for the round pipe flow seem to be identical to those for the flat channel flow.

Fig. 3 illustrates the effect of particle inertia on the particle fluctuating velocity intensity and concentration in the near-wall region of flat and round channels, when using (24) for T_{L+}. From Fig. 3(a), one can see a pronounced maximum of v'_{y+} near the wall as a function of τ_+. The initial increase in fluctuating velocity with particle inertia is due to the diffusion transport of fluctuations from the high-turbulence channel core to the low-turbulence near-wall region. The subsequent decrease in v'_{y+} beyond the maximum is explained by a reduction in the response of large particles to turbulent velocity fluctuations of the carrier fluid. The asymptotic dependence of $v'_{y+}(\tau_+)$ when $\tau_+ \to \infty$ is given by (26) and is shown in Fig. 3(a) by curves 5 and 6. As is clear from Fig. 3(b), the particle concentration increases sharply with particle inertia and peaks as well. However, the peak of Φ corresponds to less values of τ_+ as compared to the maximum of v'_{y+}. In accordance with (25) and (26), the zero-inertia

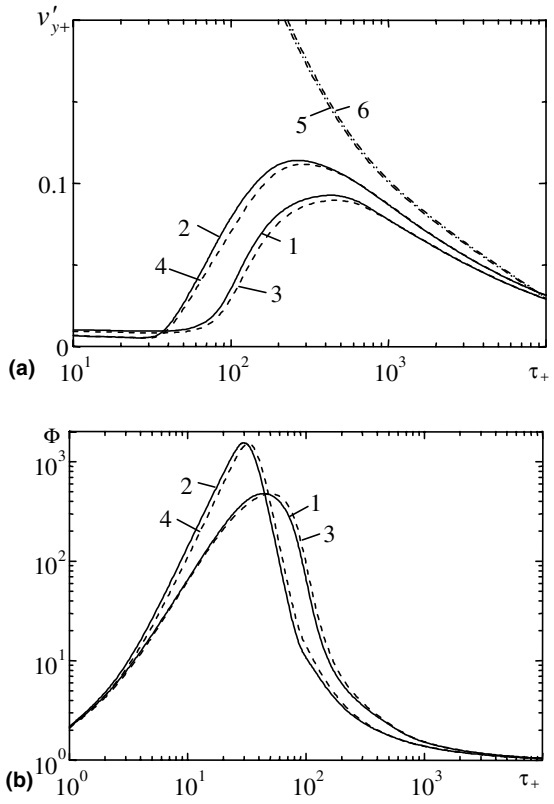

Fig. 3. Influence of particle inertia on particle fluctuating velocity (a) and concentration (b) for $y_+ = 1$: (1), (3) and (5) flat channel; (2), (4) and (6) round pipe; (1) and (2) predictions with the "transport term" in (8); (3) and (4) predictions without the "transport term" in (8); (5) and (6) formula (26).

and high-inertia particles are uniformly distributed in space and their normalized concentration is equal to unity. Fig. 3 also represents the results obtained in the absence of the "transport term" in (8). These follow from (20)–(22) when taking $f_{u1} = 0$ in (21). Obviously, the impact of the "transport term" plays a little part in increasing v'_{y+} and Φ near the wall due to some contribution to the diffusion transport of velocity fluctuations.

4. Two-point PDF model

Let us now consider the two-point PDF model. This model is suitable for predicting two-particle statistics and particle-pair dispersion in homogeneous isotropic turbulence.

Eq. (1) for two separate particles provide the equations describing the relative motion of a particle pair

$$\frac{\mathrm{d}\mathbf{r}_p}{\mathrm{d}t} = \mathbf{w}_p, \quad \frac{\mathrm{d}\mathbf{w}_p}{\mathrm{d}t} = \frac{\Delta\mathbf{u}(\mathbf{r}_p, t) - \mathbf{w}_p}{\tau_p}. \tag{27}$$

Here $\mathbf{r}_p \equiv \mathbf{R}_{p2} - \mathbf{R}_{p1}$ and $\mathbf{w}_p \equiv \mathbf{v}_{p2} - \mathbf{v}_{p1}$ denote the separation distance and the relative velocity between two particles, whereas $\Delta\mathbf{u}(\mathbf{r}_p, t) \equiv \mathbf{u}(\mathbf{R}_{p2}, t) - \mathbf{u}(\mathbf{R}_{p1}, t)$ designates the increment in velocities at two points in which the particles are located. To proceed from stochastic equations (27) to the statistical description of the relative motion of two particles, the pair PDF is introduced

$$P_w = \langle p_w \rangle = \langle \delta(\mathbf{r} - \mathbf{r}_p(t))\delta(\mathbf{w} - \mathbf{w}_p(t)) \rangle. \tag{28}$$

The pair PDF, $P_w(\mathbf{r}, \mathbf{w}, t)$, describes the probability of finding a pair of particles separated by a distance $\mathbf{r}$, with a relative velocity $\mathbf{w}$, at time t. Differentiating (28) with respect to time and accounting for (27), we derive the following equation for the pair PDF:

$$\frac{\partial P_w}{\partial t} + w_k \frac{\partial P_w}{\partial r_k} + \frac{1}{\tau_p} \frac{\partial (\Delta U_k - w_k) P_w}{\partial w_k} = -\frac{1}{\tau_p} \frac{\partial \langle \Delta u'_k p_w \rangle}{\partial w_k}. \tag{29}$$

To determine the correlation $\langle \Delta u'_k p_w \rangle$, which describes eddy–particle interactions, the fluid relative velocity field is modeled by a Gaussian random process with known two-point correlation moments. Then, by making use of the Furutsu–Donsker–Novikov formula for Gaussian random functions (Frisch, 1995), we can obtain

$$\begin{aligned} \langle \Delta u'_i p_w \rangle &= \int\int \langle \Delta u'_i(\mathbf{r}, t) \Delta u'_k(\mathbf{r}_1, t_1) \rangle \\ &\quad \times \left\langle \frac{\delta p_w(\mathbf{r}, t)}{\delta \Delta u_k(\mathbf{r}_1, t_1) \mathrm{d}\mathbf{r}_1 \, \mathrm{d}t_1} \right\rangle \mathrm{d}\mathbf{r}_1 \, \mathrm{d}t_1, \\ \left\langle \frac{\delta p(\mathbf{r}, t)}{\delta \Delta u_k(\mathbf{r}_1, t_1) \mathrm{d}\mathbf{r}_1 \, \mathrm{d}t_1} \right\rangle &= -\frac{\partial}{\partial r_j} \left\langle p(\mathbf{r}, t) \frac{\delta r_{pj}(t)}{\delta \Delta u_k(\mathbf{r}_1, t_1) \mathrm{d}\mathbf{r}_1 \, \mathrm{d}t_1} \right\rangle \\ &\quad - \frac{\partial}{\partial w_j} \left\langle p(\mathbf{r}, t) \frac{\delta w_{pj}(t)}{\delta \Delta u_k(\mathbf{r}_1, t_1) \mathrm{d}\mathbf{r}_1 \, \mathrm{d}t_1} \right\rangle. \end{aligned} \tag{30}$$

To find the functional derivatives in (30) we use the solutions of Eq. (27)

$$\begin{aligned} \mathbf{r}_p(t) &= \int_0^t \mathbf{w}_p(t_1) \mathrm{d}t_1, \\ \mathbf{w}_p(t) &= \int_0^t \varphi(t - t_1) \Delta\mathbf{u}(\mathbf{r}_p(t_1), t_1)) \mathrm{d}t_1. \end{aligned} \tag{31}$$

In what follows, applying the functional operator to (31), employing the iteration procedure, and averaging the functional derivatives over the particle probability density p_w, we represent (30) in the form similar to (7)

$$\begin{aligned} \langle \Delta u'_i p_w \rangle &= -\int_{t_1}^t \langle \Delta u'_i(\mathbf{r}, t) \Delta u'_j(\mathbf{r}_p(t_1), t_1) \rangle \\ &\quad \times \int_{t_1}^t \varphi(t - t_2) \mathrm{d}t_2 \, \mathrm{d}t_1 \frac{\partial P_w}{\partial r_j} \\ &\quad - \int_{t_1}^t \langle \Delta u'_i(\mathbf{r}, t) \Delta u'_k(\mathbf{r}_p(t_1), t_1) \rangle \\ &\quad \times \left[\delta_{jk} \varphi(t - t_1) + \frac{\partial \Delta U_j}{\partial r_k} \int_{t_1}^t \varphi(t - t_2) \right. \\ &\quad \left. \times \int_{t_1}^{t_2} \varphi(t_2 - t_3) \mathrm{d}t_3 \, \mathrm{d}t_2 \right] \mathrm{d}t_1 \frac{\partial P_w}{\partial w_j}. \end{aligned} \tag{32}$$

In order to represent the integrals in (32) in an explicit form, the Lagrangian two-point structure function of fluid velocities is approximated in the same way as (8)

$$S_{\mathrm{L}ij}(\mathbf{r},t,\tau) = \langle (u_i'(\mathbf{R}_2(t),t) - u_i'(\mathbf{R}_1(t),t))(u_j'(\mathbf{R}_2(t-\tau), t-\tau) - u_j'(\mathbf{R}_1(t-\tau),t-\tau)) \mid \mathbf{r} = \mathbf{R}_2(t) - \mathbf{R}_1(t)\rangle = \left(S_{ij} - \frac{\tau}{2}\frac{DS_{ij}}{Dt}\right)\Psi_{\mathrm{L}r}(\tau \mid r), \tag{33}$$

$$\frac{DS_{ij}}{Dt} = \frac{\partial S_{ij}}{\partial t} + \Delta U_k \frac{\partial S_{ij}}{\partial r_k} + \frac{\partial S_{ijk}}{\partial r_k},$$

where the second- and third-order Eulerian structure functions are defined as

$$S_{ij}(\mathbf{r},t) = \langle \Delta u_i' \Delta u_j' \rangle = \langle (u_i'(\mathbf{x}+\mathbf{r},t) - u_i'(\mathbf{x},t))(u_j'(\mathbf{x}+\mathbf{r},t) - u_j'(\mathbf{x},t))\rangle,$$

$$S_{ijk}(\mathbf{r},t) = \langle \Delta u_i' \Delta u_j' \Delta u_k' \rangle = \langle (u_i'(\mathbf{x}+\mathbf{r},t) - u_i'(\mathbf{x},t))(u_j'(\mathbf{x}+\mathbf{r},t) - u_j'(\mathbf{x},t)) \times (u_k'(\mathbf{x}+\mathbf{r},t) - u_k'(\mathbf{x},t))\rangle.$$

In (33), $\Psi_{\mathrm{L}r}(\tau|r)$ symbolizes a Lagrangian autocorrelation function that describes the velocity increments of two fluid elements separated initially by the distance r. Like (8), approximation (33) contains the "transport term" that accounts for the effects of turbulence unsteadiness as well as of the convective and diffusive transfer of fluid velocity fluctuations along a particle-pair trajectory. Substitution of (33) into (32) provides the following equation for the correlation between the fluid velocity increment and the particle-pair probability density:

$$\langle \Delta u_i' p_w \rangle = -S_{ij}\left(f_r \frac{\partial P_w}{\partial w_j} + \tau_p g_r \frac{\partial P_w}{\partial r_j}\right) + \frac{\tau_p f_{r1}}{2}\frac{DS_{ij}}{Dt}\frac{\partial P_w}{\partial w_j} - \tau_p l_r S_{ik}\frac{\partial \Delta U_j}{\partial r_k}\frac{\partial P_w}{\partial w_j},$$

$$f_r = \frac{1}{\tau_p}\int_0^\infty \Psi_{\mathrm{L}r}(\tau)\exp\left(-\frac{\tau}{\tau_p}\right)\mathrm{d}\tau, \quad g_r = \frac{T_{\mathrm{L}r}}{\tau_p} - f_r,$$

$$f_{r1} = \frac{1}{\tau_p^2}\int_0^\infty \Psi_{\mathrm{L}r}(\tau)\tau\exp\left(-\frac{\tau}{\tau_p}\right)\mathrm{d}\tau, \quad l_r = g_r - f_{r1}. \tag{34}$$

The coefficients f_r, g_r, f_{r1}, l_r quantify a response of a pair of particles, separated by the distance r, to velocity fluctuations of the turbulent fluid, and $T_{\mathrm{L}r} \equiv \int_0^\infty \Psi_{\mathrm{L}r}(\tau)\mathrm{d}\tau$. When the distance between particles increases, the following limits take place:

$$\Psi_{\mathrm{L}r}(\tau \mid r) = \Psi_{\mathrm{L}}(\tau), \quad T_{\mathrm{L}r} = T_{\mathrm{L}}, \quad f_r = f_u, \quad g_r = g_u, \quad f_{r1} = f_{u1}, \quad l_r = l_u \quad \text{for } r \to \infty.$$

The exponential approximation, $\Psi_{\mathrm{L}r} = \exp(-\tau/T_{\mathrm{L}r})$, yields the response coefficients akin to (11)

$$f_r = \frac{T_{\mathrm{L}r}}{\tau_p + T_{\mathrm{L}r}}, \quad g_r = \frac{T_{\mathrm{L}r}^2}{\tau_p(\tau_p + T_{\mathrm{L}r})}, \quad f_{r1} = \frac{T_{\mathrm{L}r}^2}{(\tau_p + T_{\mathrm{L}r})^2}, \quad l_r = \frac{T_{\mathrm{L}r}^3}{\tau_p(\tau_p + T_{\mathrm{L}r})^2}. \tag{35}$$

Substituting (34) into (29) yields the following kinetic equation for the two-point PDF of the particle-pair relative velocity distribution in homogeneous isotropic turbulence

$$\frac{\partial P_w}{\partial t} + w_k\frac{\partial P_w}{\partial r_k} + \frac{1}{\tau_p}\frac{\partial(\Delta U_k - w_k)P_w}{\partial w_k} + \frac{f_{r1}}{2}\frac{DS_{ik}}{Dt}\frac{\partial^2 P_w}{\partial w_i \partial w_k} = S_{ik}\left(\frac{f_r}{\tau_p}\frac{\partial^2 P_w}{\partial w_i \partial w_k} + g_r\frac{\partial^2 P_w}{\partial r_i \partial w_k} + l_r\frac{\partial \Delta U_n}{\partial r_k}\frac{\partial^2 P_w}{\partial w_i \partial w_n}\right). \tag{36}$$

Eq. (36) describes the convective and diffusive transport in phase space $(\mathbf{r},\mathbf{w})$ and resembles the one-point PDF equation (12). However, the one-point and two-point kinetic equations bear a superficial resemblance, because (12) deals with the one-particle PDF and hence does not take into consideration the spatial correlation of the motion of two particles. In contrast, the two-point statistical model allows for the spatial correlation between the velocities of particle pairs and thereby can predict the effect of clustering. When $DS_{ij}/Dt = \Delta\mathbf{U} = 0$, (36) reduces to the two-point PDF equation obtained in Zaichik and Alipchenkov (2003).

Eq. (36) generates a set of balance equations governing the pair concentration, momentum, particulate stresses, or any appropriate statistical two-point moments of the relative velocity PDF. By this means the equations describing the particle-pair density, the mean relative velocity, and the second-order two-point structure function are written as

$$\frac{\partial N}{\partial t} + \frac{\partial N W_k}{\partial r_k} = 0, \tag{37}$$

$$\frac{\partial W_i}{\partial t} + W_k\frac{\partial W_i}{\partial r_k} = -\frac{\partial S_{pik}}{\partial r_k} + \frac{\Delta U_i - W_i}{\tau_p} - \frac{D_{pik}^r}{\tau_p}\frac{\partial \ln N}{\partial r_k}, \tag{38}$$

$$\frac{\partial S_{pij}}{\partial t} + W_k\frac{\partial S_{pij}}{\partial r_k} + \frac{1}{N}\frac{\partial N S_{pijk}}{\partial r_k} + f_{r1}\frac{DS_{ij}}{Dt} = -(S_{pik} + g_r S_{ik})\frac{\partial W_j}{\partial r_k} - (S_{pjk} + g_r S_{jk})\frac{\partial W_i}{\partial r_k} + l_r\left(S_{ik}\frac{\partial \Delta U_j}{\partial r_k} + S_{jk}\frac{\partial \Delta U_i}{\partial r_k}\right) + \frac{2}{\tau_p}(f_r S_{ij} - S_{pij}), \tag{39}$$

where

$$N = \int P_w \mathrm{d}\mathbf{w}, \quad W_i = \frac{1}{N}\int w_i P_w \mathrm{d}\mathbf{w}, \quad S_{pij} = \langle w_i' w_j' \rangle = \frac{1}{N}\int (w_i - W_i)(w_j - W_j) P_w \mathrm{d}\mathbf{w},$$

$$S_{pijk} = \langle w'_i w'_j w'_k \rangle = \frac{1}{N} \int (w_i - W_i)(w_j - W_j)(w_k - W_k) P_w \, \mathrm{d}\mathbf{w},$$

$$D^r_{pij} = \tau_p (S_{pij} + g_r S_{ij}).$$

The third-order particle structure function is determined by the gradient relation that is akin to (16)

$$S_{pijk} = -\frac{1}{3}\left(D^r_{pin} \frac{\partial S_{pjk}}{\partial r_n} + D^r_{pjn} \frac{\partial S_{pik}}{\partial r_n} + D^r_{pkn} \frac{\partial S_{pij}}{\partial r_n} \right). \tag{40}$$

In the zero-inertia limit, conformity with (39), the second-order structure functions of both phases are equal

$$\lim_{\tau_p \to 0} S_{pij} = S_{ij}, \tag{41}$$

and the pair diffusivity tensor of fine particles coincides with that of fluid elements

$$\lim_{\tau_p \to 0} D^r_{pij} = D^r_{ij} = T_{\mathrm{L}r} S_{ij}. \tag{42}$$

In accordance with (40)–(42), the third-order structure function of fluid fluctuating velocities is given by

$$S_{ijk} = \lim_{\tau_p \to 0} S_{pijk} = -\frac{T_{\mathrm{L}r}}{3}\left(S_{in} \frac{\partial S_{jk}}{\partial r_n} + S_{jn} \frac{\partial S_{ik}}{\partial r_n} + S_{kn} \frac{\partial S_{ij}}{\partial r_n} \right). \tag{43}$$

5. Particle dispersion in isotropic turbulence

The two-point PDF model is used for predicting pair dispersion in a steady-state suspension of particles immersed in homogeneous, isotropic, and stationary turbulence. In isotropic turbulence, due to spherical symmetry, the pair relative velocity and density distributions are independent of the orientation of the separation vector $\mathbf{r}$ and may be only dependent on $r = |\mathbf{r}|$. In addition, the convective transport in the fluid is supposed to be absent ($\Delta U_i = 0$), and the total number of particles is not changed in time. The latter infers that the balance between the net radial relative inward and out ward fluxes takes place, and, therefore, the mean relative velocity, W_r, is equal to zero. By this means the set of Eqs. (37)–(40) along with (43) is constricted to the following system:

$$\frac{2(\overline{S}_{pll} - \overline{S}_{pnn})}{\bar{r}} + \frac{\mathrm{d}\overline{S}_{pll}}{\mathrm{d}\bar{r}} + (\overline{S}_{pll} + g_r \overline{S}_{ll}) \frac{\mathrm{d} \ln \Gamma}{\mathrm{d}\bar{r}} = 0, \tag{44}$$

$$St^2 \frac{\mathrm{d}}{\mathrm{d}\bar{r}}\left[\Gamma(\overline{S}_{pll} + g_r \overline{S}_{ll}) \frac{\mathrm{d}\overline{S}_{pll}}{\mathrm{d}\bar{r}} \right] + St f_{r1} \Gamma \frac{\mathrm{d}}{\mathrm{d}\bar{r}}\left(\overline{T}_{\mathrm{L}r} \overline{S}_{ll} \frac{\mathrm{d}\overline{S}_{ll}}{\mathrm{d}\bar{r}} \right) + 2\Gamma(f_r \overline{S}_{ll} - \overline{S}_{pll}) = 0, \tag{45}$$

$$\frac{St^2}{3\bar{r}^2}\left\{ \frac{\mathrm{d}}{\mathrm{d}\bar{r}}\left[\bar{r}^2 \Gamma(\overline{S}_{pll} + g_r \overline{S}_{ll}) \frac{\mathrm{d}\overline{S}_{pnn}}{\mathrm{d}\bar{r}} \right] + 2\frac{\mathrm{d}}{\mathrm{d}\bar{r}}\left[\bar{r}\Gamma(\overline{S}_{pnn} + g_r \overline{S}_{nn})(\overline{S}_{pll} - \overline{S}_{pnn}) \right] \right\} + \frac{St f_{r1} \Gamma}{3\bar{r}^2}\left\{ \frac{\mathrm{d}}{\mathrm{d}\bar{r}}\left(\bar{r}^2 \overline{T}_{\mathrm{L}r} \overline{S}_{ll} \frac{\mathrm{d}\overline{S}_{nn}}{\mathrm{d}\bar{r}} \right) + 2\frac{\mathrm{d}}{\mathrm{d}\bar{r}}\left[\bar{r} \overline{T}_{\mathrm{L}r} \overline{S}_{nn}(\overline{S}_{ll} - \overline{S}_{nn}) \right] \right\} + 2\Gamma(f_r \overline{S}_{nn} - \overline{S}_{pnn}) = 0. \tag{46}$$

In (44)–(46), the overbar stands for normalization by the Kolmogorov microscales, St is the Stokes number that specifies the particle inertia, Γ is the radial distribution function that quantifies the accumulation effect, S_{pll} and S_{pnn} are the longitudinal and transverse components of the particle velocity structure function S_{pij}. Thus the model under consideration amounts to solving three nonlinear ordinary differential equations involving the radial distribution function and the second-order longitudinal and transverse structure functions. Like (20), Eq. (44) expresses the balance between the turbophoretic and diffusion forces in the separation direction between two particles.

Relevant boundary conditions for Eqs. (44)–(46) are given by

$$\frac{\mathrm{d}\overline{S}_{pll}}{\mathrm{d}\bar{r}} = \frac{\mathrm{d}\overline{S}_{pnn}}{\mathrm{d}\bar{r}} = 0 \quad \text{for } \bar{r} = 0, \tag{47}$$

$$\overline{S}_{pll} = f_u \overline{S}_{ll}, \quad \overline{S}_{pnn} = f_u \overline{S}_{nn}, \quad \Gamma = 1 \quad \text{for } \bar{r} \to \infty. \tag{48}$$

Conditions (47) express the balance between the radial relative inward and outward fluxes at the origin, and they are valid if the particle size is less than the Kolmogorov length microscale. Relations (48) point to the fact that the particle velocities become near-homogeneous at large separation, whereas the particles are randomly distributed.

To determine the structure functions of fluid velocity fluctuations, S_{ll} and S_{nn}, as well as the two-point velocity increment timescale, $T_{\mathrm{L}r}$, we consider the behaviour of these quantities in the viscous, inertial, and external spatial subranges of separation. In the viscous range ($r \leqslant \eta$), the first terms of the Taylor expansion of the Eulerian velocity structure functions are the following (Monin and Yaglom, 1975):

$$S_{ll} = \frac{\varepsilon r^2}{15\nu}, \quad S_{nn} = \frac{2\varepsilon r^2}{15\nu}. \tag{49}$$

According to (42) and (49), the longitudinal and transverse pair diffusivities of fluid elements are given by

$$D^r_{ll} = \frac{\varepsilon T_{\mathrm{L}r} r^2}{15\nu}, \quad D^r_{nn} = \frac{2\varepsilon T_{\mathrm{L}r} r^2}{15\nu}. \tag{50}$$

Expressions (50) agree with the turbulent pair diffusivities derived by Lundgren (1981) when taking

$$T_{Lr} = \tau_\sigma = A_1\tau_k, \quad A_1 = 5^{1/2}. \tag{51}$$

In the inertial range ($\eta \ll r \ll L$), Kolmogorov's similarity hypotheses give the following scaling for the second-order structure functions (Monin and Yaglom, 1975):

$$S_{ll} = C(\varepsilon r)^{2/3}, \quad S_{nn} = \frac{4}{3}C(\varepsilon r)^{2/3}, \quad C \approx 2.0. \tag{52}$$

In the inertial range, the only time scale can be built up, that is $\varepsilon^{-1/3}r^{2/3}$, and, therefore, the two-point timescale has to be taken in the form

$$T_{Lr} = A_2\varepsilon^{-1/3}r^{2/3}, \quad A_2 = \text{const}. \tag{53}$$

In what follows, according to (43), the longitudinal third-order structure function of fluid fluctuating velocities is determined as

$$S_{lll} = -T_{Lr}S_{ll}\frac{\mathrm{d}S_{ll}}{\mathrm{d}r}. \tag{54}$$

Substituting (52) and (53) into (54) yields

$$S_{lll} = -\frac{2}{3}A_2C^2\varepsilon r. \tag{55}$$

On the other hand, the longitudinal third-order structure function in the inertial subrange is defined by the well-known Kolmogorov relation (Monin and Yaglom, 1975)

$$S_{lll} = -\frac{4}{5}\varepsilon r \tag{56}$$

and thus, from the comparison of (55) and (56), we obtain $A_2 = 0.3$ when $C = 2.0$.

The fluid velocities at two points separated by large distance are statistically independent. Therefore, in the external range ($r > L$), the structure functions are as follows:

$$S_{ll} = S_{nn} = 2u'^2. \tag{57}$$

Moreover, when the separation r exceeds the integral length scale L, the two-point timescale goes over into the conventional Lagrangian integral timescale

$$T_{Lr} = T_L. \tag{58}$$

By this means, the fluid velocity structure functions are given by the approximations

$$\frac{1}{\overline{S}_{ll}^k} = \left(\frac{15}{\bar{r}^2}\right)^k + \frac{1}{(C\bar{r}^{2/3})^k} + \left(\frac{15^{1/2}}{2Re_\lambda}\right)^k,$$
$$\frac{1}{\overline{S}_{nn}^k} = \left(\frac{15}{2\bar{r}^2}\right)^k + \left(\frac{3}{4C\bar{r}^{2/3}}\right)^k + \left(\frac{15^{1/2}}{2Re_\lambda}\right)^k,$$
$$C = 2, \quad k = 20, \tag{59}$$

which interpolate (49), (52) and (57) with Re_λ being the Reynolds number based on the Taylor length scale.

In the similar way, the two-point timescale is taken by combining (51), (53) and (58) as follows:

$$\frac{1}{\overline{T}_{Lr}^k} = \frac{1}{A_1^k + (A_2\bar{r}^{2/3})^k} + \frac{1}{\overline{T}_L^k}, \quad A_1 = 5^{1/2}, \ A_2 = 0.3. \tag{60}$$

Approximations (59) and (60) are identical to those taken in Zaichik and Alipchenkov (2003), except for the value of the constant A_2, which is modified here in order to satisfy Kolmogorov's relation (56). In (60), the Lagrangian integral timescale normalized by the Kolmogorov microscale is determined by the following equation:

$$\overline{T}_L = \frac{T_L}{\tau_k} = \frac{2(\mathrm{Re}_\lambda + C_1)}{15^{1/2}C_{0\infty}}, \quad C_{0\infty} = 7, \ C_1 = 32,$$

which approximates DNS data by Yeung and Pope (1989), Yeung (1997), Yeung (2001), and Février et al. (2001) with the asymptotic value of the Kolmogorov constant $C_{0\infty}$ recommended by Sawford (1991).

Eqs. (44)–(46) along with boundary conditions (47) and (48) were solved numerically, and the results obtained were compared with DNS computations by Sundaram and Collins (1997) and Wang et al. (2000). However, before presenting numerical results, let us consider the asymptotic solutions to this problem in the zero- and high-inertia limits. In the zero-inertia limit ($St = 0$, $f_r = 1$), it follows from (44)–(46):

$$\overline{S}_{pll} = \overline{S}_{ll}, \quad \overline{S}_{pnn} = \overline{S}_{nn}, \quad \Gamma = 1. \tag{61}$$

According to (61), zero-inertia particles entirely follow the fluid turbulent velocities and are uniformly distributed in space.

In the high-inertia limit, it is easy to obtain the following solution:

$$\overline{S}_{pll} = \overline{S}_{pnn} = \frac{2\overline{T}_L Re_\lambda}{15^{1/2}St}, \quad \Gamma = 1, \tag{62}$$

which resembles solution (26) for channel flow.

Fig. 4 shows the particle structure and radial distribution functions predicted for various Stokes numbers against the separation distance. As can be observed, these distributions remind the appropriate profiles of the particle fluctuating velocity and concentration across the channel section (Figs. 1 and 2). With increasing St, the particle structure functions deviate more and more from those in the fluid (curves 1) and approach to the homogeneous asymptotic distributions given by (62) for high-inertia particles. Although the fluid velocity structure functions are equal to zero at $\bar{r} = 0$, the structure functions of fairly inertial particles, by virtue of diffusion transfer, have non-zero values at the origin. Due to the turbophoretic force, the radial distribution function monotonically rises with decreasing separation distance. It is also seen from Fig. 4(c) that the radial distribution function of low-inertia particles, like the

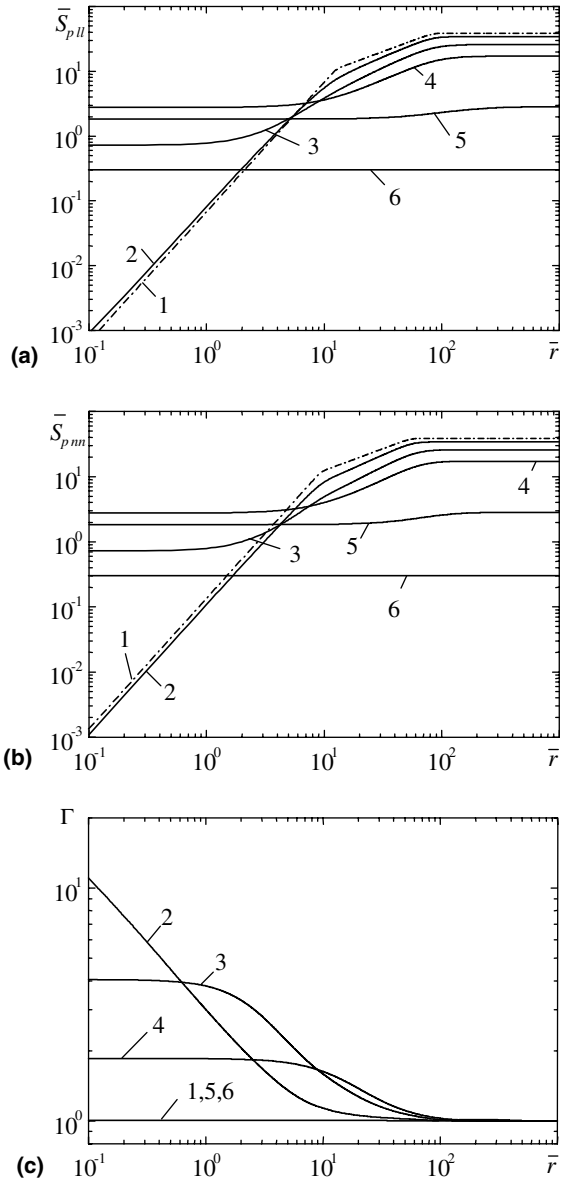

Fig. 4. The longitudinal (a) and transverse (b) structure functions and the radial distribution function (c) for $Re_\lambda = 75$: (1) $St = 0$, (2) 1, (3) 4, (4) 10, (5) 100 and (6) 1000.

particle concentration on the channel wall, has a singularity at $\bar{r} = 0$. As the Stokes number increases, this singularity disappears and Γ tends to unity.

Fig. 5 demonstrates the ratio between the particle transverse and longitudinal structure functions for $\bar{r} = 1$ versus the Stokes number. For fluid elements as well as for zero-inertia particles, this ratio is two in conformity with (49). In accordance with the DNS data of Wang et al. (2000), the predicted ratio of S_{pnn}/S_{pll} drops quickly towards one as St increases. Because of decreasing the role of the diffusion transfer of velocity fluctuations, the ratio predicted with no the "transport term" in (33), i.e. when taking $f_{r1} = 0$ in (45) and (46), is found to approach unity not so quickly as the DNS results.

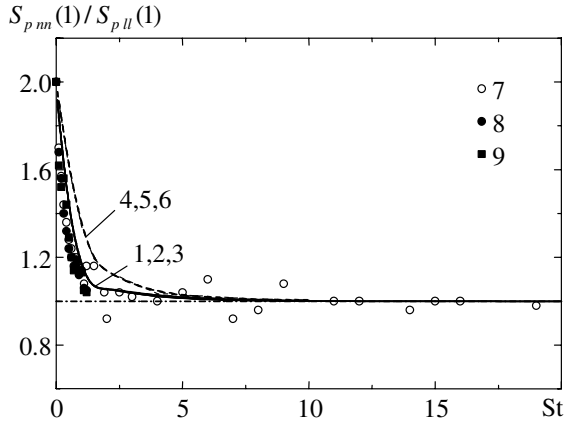

Fig. 5. Ratio between the transverse and longitudinal structure functions for $\bar{r} = 1$: (1)–(3) predictions with the "transport term" in (33); (4)–(6) predictions without the "transport term" in (33); (7)–(9) DNS by Wang et al. (2000); (1), (4) and (7) $Re_\lambda = 24$; (2), (5) and (8) $Re_\lambda = 45$; (3), (6) and (9) $Re_\lambda = 75$.

In Fig. 6, we compare the mean radial relative velocities predicted from (44)–(48) with numerical simulations by Wang et al. (2000). Under the assumption that the PDF of the relative velocity is Gaussian, the mean relative velocity magnitude is defined in terms of the longitudinal structure function as $\langle | \bar{w}_r | \rangle = (2\overline{S}_{pll}/\pi)^{1/2}$. Fig. 6 illustrates the influence of particle inertia on $\langle | \bar{w}_r | \rangle$ over a wide range of Stokes numbers. As is clear, the behaviour of $\langle | \bar{w}_r | \rangle$, with respect to St, is qualitatively similar to that of v'_{y+} depending on τ_+ (Fig. 3(a)) and is characterized by the presence of maximum. The initial rise in $\langle | \bar{w}_r | \rangle$ is attributable to a decrease in the correlation of particle velocities with τ_p. The subsequent decay of $\langle | \bar{w}_r | \rangle$ beyond the maximum results from a decrease in the particle fluctuating velocities, since the particles become more sluggish and less

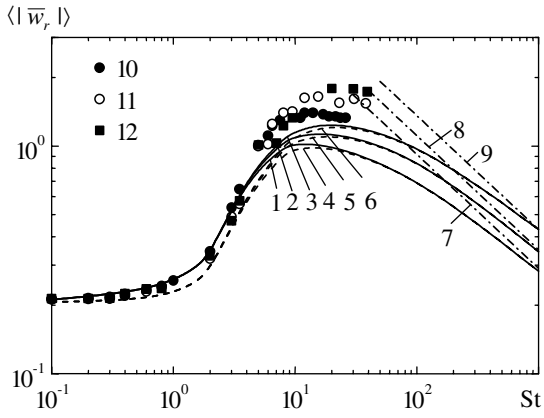

Fig. 6. Influence of particle inertia on the mean relative velocity magnitude for $\bar{r} = 1$: (1)–(3) predictions with the "transport term" in (33); (4)–(6) predictions without the "transport term" in (33); (7)–(9) (63); (10)–(12) DNS by Wang et al. (2000); (1), (4), (7) and (10) $Re_\lambda = 45$; (2), (5), (8) and (11) $Re_\lambda = 58$; (3), (6), (9) and (12) $Re_\lambda = 75$.

responsive to the fluid turbulence. In the limit of high-inertia particles ($St \to \infty$), $\langle | \bar{w}_r | \rangle$ is determined by the relation

$$\langle | \bar{w}_r | \rangle = \frac{2}{15^{1/2}} \left(\frac{\overline{T}_{\mathrm{L}} Re_\lambda}{\pi St} \right)^{1/2}, \tag{63}$$

which follows from (62). From Fig. 6, it is also seen that the additional diffusion transfer caused by the "transport term" in (33) leads to a slight increase in mean relative velocities of low-inertia particles.

Fig. 7 shows the influence of particle inertia on the radial distribution function for separation distances and Reynolds numbers, which correspond to the DNS data of Sundaram and Collins (1997) and Wang et al. (2000). This influence is reminiscent of the effect of particle inertia on the concentration near the wall of a channel (Fig. 3(b)). As expected, in the limiting cases of zero-inertia and high-inertia particles, the concentration field is statistically uniform, and therefore the radial distribution function is equal to unity. In accordance with the computations, the predicted radial distribution function goes through a peak as the particle inertia time increases. Thus there exists a critical particle response time which results in maximum preferential concentration. The value of this critical response time is of the same order as the Kolmogorov timescale. Fig. 7 also exhibits that the impact of the additional diffusion due to the "transport term", like the particle accumulation in the viscous sublayer of a channel flow, results in increasing preferential concentration.

Finally let us consider the effect of particle inertia on the collision rate that is derived from the relationship

$$\beta = 2\pi\sigma^2 \langle | w_r(\sigma) | \rangle \Gamma(\sigma) = (8\pi S_{pll}(\sigma))^{1/2} \sigma^2 \Gamma(\sigma), \tag{64}$$

where σ is the radius of a collision sphere which is equal to the particle diameter for identical particles. It is clear from (64) that the turbulence-induced collision rate is governed by the mean relative velocity as well as by the radial distribution function. Consequently, the interaction of particles with turbulent eddies causes two statistical mechanisms which contribute to the collision rate, namely, the relative velocity between neighboring particles (the turbulent transport effect) and the non-uniform particle distribution (the accumulation effect). Substituting asymptotic solutions (61) and (62) into (64) produce, respectively, the collision rates in the limits of zero-inertia and high-inertia particles. By this means (61) and (64) along with (49) lead to the well-known collision kernel of Saffman and Turner (1956) for fine particles ($\tau_p \ll \tau_k$)

$$\beta_{\mathrm{ST}} = \left(\frac{8\pi\varepsilon}{15\nu} \right)^{1/2} \sigma^3. \tag{65}$$

Relations (62) and (64) entail the collision kernel for coarse particles ($\tau_p \gg T_{\mathrm{L}}$)

$$\beta = \left(\frac{8\pi T_{\mathrm{L}} u'^2}{\tau_p} \right)^{1/2} \sigma^2. \tag{66}$$

As is evident from (65) and (66), the collision rate of both fine and coarse particles is governed solely by the turbulent transport mechanism. However, the accumulation effect is extremely important when the particle relaxation time is comparable with the Kolmogorov time microscale.

Fig. 8 represents the collision kernel normalized with the Saffman–Turner one and compares predictions with DNS data by Wang et al. (2000). As seen, the model accounting for the "transport term" in (33) properly captures the crucial trends of the DNS results, although the predicted maxima of β are slightly shifted towards particles with larger inertia. The collision kernels, predicted with no the "transport term" (i.e. when taking $f_{r1} = 0$), are smaller in values and worse correspond to

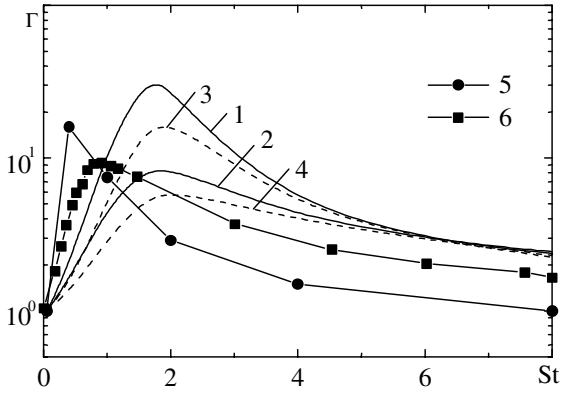

Fig. 7. Influence of particle inertia on the radial distribution function: (1) and (2) predictions with the "transport term" in (33); (3) and (4) predictions without the "transport term" in (33); (5) DNS by Sundaram and Collins (1997); (6) DNS by Wang et al. (2000); (1), (3), (5) $\bar{r} = 0.36$, $Re_\lambda = 54$; (2), (4) and (6) $\bar{r} = 1$, $Re_\lambda = 58$.

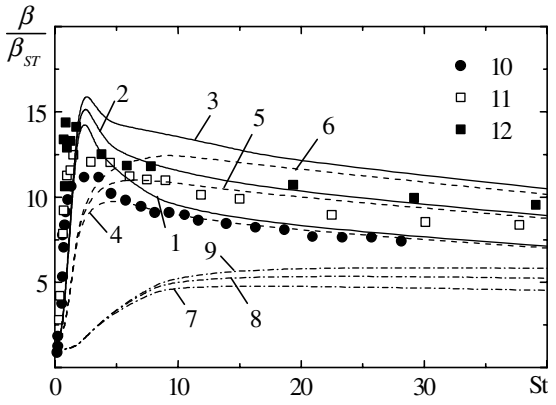

Fig. 8. Influence of particle inertia on the collision kernel for $\sigma = 1$: (1)–(3) predictions with the "transport term" in (33); (4)–(6) predictions without the "transport term" in (33); (7)–(9) predictions for $\Gamma = 1$; (10)–(12) DNS by Wang et al. (2000); (1), (4), (7), (10) $Re_\lambda = 45$; (2), (5), (8), (11) $Re_\lambda = 58$; (3), (6), (9) and (12) $Re_\lambda = 75$.

the DNS than those obtained using the full model. In Fig. 8, it is also depicted the collision rate predicted without the effect of preferential concentration, when the radial distribution function is assumed to be equal to unity. It is clear that the neglect of preferential concentration leads to considerably less values of the collision rate than those given by the DNS.

6. Summary

Two statistical models for predicting particle dispersion and preferential concentration in inhomogeneous sheared and homogeneous isotropic turbulent flows are presented. These models are based on the one-point and two-point PDFs of particle velocity distributions in Gaussian random fluid flow fields.

The one-point model is used to analyse the fluctuating velocity and the concentration of particles in near-wall channel flows, whereas the two-point model is employed to predict the relative velocity and the radial distribution function of particle-pairs in homogeneous isotropic turbulence.

A unified approach to modelling particle preferential concentration in inhomogeneous and homogeneous turbulent flow fields is demonstrated by treating this phenomenon as a particle migration caused by the turbophoretic force. This approach captures the accumulation of inertial particles in both near-wall and isotropic turbulence reasonably well.

References

Balkovsky, E., Falkovich, G., Fouxon, A., 2001. Intermittent distribution of inertial particles in turbulent flows. Phys. Rev. Lett. 86 (13), 2790–2793.

Bec, J., 2003. Fractal clustering of inertial particles in random flows. Phys. Fluids 15 (11), L81–L84.

Cerbelli, S., Giusti, A., Soldati, A., 2001. ADF approach to predicting dispersion of heavy particles in wall-bounded turbulence. Int. J. Multiphase Flow 27, 1861–1879.

Chen, M., Kontomaris, K., McLaughlin, J.B., 1998. Direct numerical simulation of droplet collisions in a turbulent channel flow. Part II: collision rates. Int. J. Multiphase Flow 24, 1105–1138.

Derevich, I.V., 2000. Statistical modelling of mass transfer in turbulent two-phase dispersed flows. 1. Model development. Int. J. Heat Mass Transfer 43 (19), 3709–3723.

Derevich, I.V., Zaichik, L.I., 1988. Particle deposition from a turbulent flow. Fluid Dynam. 23 (5), 722–729.

Elperin, T., Kleeorin, N., L'vov, V.S., Rogachevskii, I., Sokoloff, D., 2002. Clustering instability of the spatial distribution of inertial particles in turbulent flows. Phys. Rev. E 66 (036302), 1–16.

Fessler, J.R., Kulick, J.D., Eaton, J.K., 1994. Preferential concentration of heavy particles in a turbulent channel flow. Phys. Fluids 6 (11), 3742–3749.

Février, P., Simonin, O., Legendre, D., 2001. Particle dispersion and preferential concentration dependence on turbulent Reynolds number from direct and large-eddy simulations of isotropic homogeneous turbulence. In: Proceedings of the Forth International Conference on Multiphase Flow, New Orleans, pp. 1–8.

Frisch, U., 1995. Turbulence. Cambridge University Press, Cambridge.

Fukagata, K., Zahrai, S., Bark, F.H., 1998. Force balance in a turbulent particulate channel flow. Int. J. Multiphase Flow 24, 867–887.

Hanjalić, K., Launder, B.E., 1972. A Reynolds stress model of turbulence and its application to thin shear flows. J. Fluid Mech. 52 (4), 609–638.

Hogan, R.C., Cuzzi, J.N., 2001. Stokes and Reynolds number dependence of preferential particle concentration in simulated three-dimensional turbulence. Phys. Fluids 13 (10), 2938–2945.

Hyland, K.E., McKee, S., Reeks, M.W., 1999. Deviation of a pdf kinetic equation for the transport of particles in turbulent flows. J. Phys. A: Math. Gen. 32, 6169–6190.

Kallio, G.A., Reeks, M.W., 1989. A numerical simulation of particle deposition in turbulent boundary layer. Int. J. Multiphase Flow 15 (3), 433–446.

Li, Y., McLaughlin, J.B., Kontomaris, K., Portela, L., 2001. Numerical simulation of particle-laden turbulent channel flow. Phys. Fluids 13 (10), 2957–2967.

Lundgren, T.S., 1981. Turbulent pair dispersion and scalar diffusion. J. Fluid Mech. 111, 27–57.

Monin, A.S., Yaglom, A.M., 1975. Statistical Fluid Mechanics: Mechanics of Turbulence, Vol. 2. MIT Press, Cambridge.

Pandya, R.V.R., Mashayek, F., 2003. Non-isothermal dispersed phase of particles in turbulent flow. J. Fluid Mech. 475, 205–245.

Portela, L.M., Cota, P., Oliemans, R.V.A., 2001. Numerical study of the near-wall behaviour of particles in turbulent pipe flows. In: Proceedings of the Fourth International Conference on Multiphase Flow, New Orleans, pp. 1–12.

Pozorrski, J., Minier, J.-P., 1999. Probability density function modeling of dispersed two-phase turbulent flows. Phys. Rev. E 59 (1), 855–863.

Reade, W.C., Collins, L.R., 2000. Effect of preferential concentration on turbulent collision rates. Phys. Fluids 12 (10), 2530–2540.

Reeks, M.W., 1977. On the dispersion of small particles suspended in an isotropic turbulent fluid. J. Fluid Mech. 83 (3), 529–546.

Reeks, M.W., 1983. The transport of discrete particles in inhomogeneous turbulence. J. Aerosol Sci. 14 (6), 729–739.

Reeks, M.W., 1991. On a kinetic equation for the transport of particles in turbulent flows. Phys. Fluids A 3 (3), 446–456.

Rouson, D.W.I., Eaton, J.K., 2001. On the preferential concentration of solid particles in turbulent channel flow. J. Fluid Mech. 428, 149–169.

Saffman, P.G., Turner, J.S., 1956. On the collision of drops in turbulent clouds. J. Fluid Mech. 1 (1), 16–30.

Sawford, B.L., 1991. Reynolds number effects in Lagrangian stochastic models of turbulent dispersion. Phys. Fluids A 3 (6), 1577–1586.

Sergeev, Y.A., Johson, R.S., Swailes, D.C., 2002. Dilute suspension of high inertia particles in the turbulent flow near the wall. Phys. Fluids 14 (3), 1042–1055.

Sigurgeirsson, H., Stuart, A.M., 2002. A model for preferential concentration. Phys. Fluids 14 (12), 4352–4361.

Simonin, O., 1991. Third-moment closure. Annexe 3, Rapport EDF HE 44/91.24.

Simonin, O., 1996. Combustion in two-phase flows: Continuum modelling of dispersed two-phase flows. Lecture Series 1996-02, Von Karman Institute for Fluid Dynamics.

Squires, K.D., Eaton, J.K., 1991. Preferential concentration of particles by turbulence. Phys. Fluids A 3 (5), 1169–1178.

Sundaram, S., Collins, L.R., 1997. Collision statistics in an isotropic particle-laden turbulent suspension. Part 1. Direct numerical simulations. J. Fluid Mech. 335, 75–109.

Swailes, D.C., Darbyshire, K.F.F., 1997. A generalized Fokker–Plank equation for particle transport in random media. Physica A 242, 38–48.

Swailes, D.C., Sergeev, Y.A., Parker, A., 1998. Chapman–Enskog closure approximation in the kinetic theory of dilute turbulent gas-particulate suspensions. Physica A 254, 517–547.

Wang, L.-P., Maxey, R.M., 1993. Settling velocity and concentration distribution of heavy particles in homogeneous isotropic turbulence. J. Fluid Mech. 256, 27–68.

Wang, L.-P., Stock, D.E., 1993. Dispersion of heavy particles in turbulent motion. J. Atmos. Sci. 50 (13), 1897–1913.

Wang, L.-P., Wexler, A.S., Zhou, Y., 2000. Statistical mechanical description and modeling of turbulent collision of inertial particles. J. Fluid Mech. 415, 117–153.

Yeung, P.K., 1997. One- and two-particle Lagrangian acceleration correlations in numerically simulated homogeneous turbulence. Phys. Fluids 9 (10), 2981–2990.

Yeung, P.K., 2001. Lagrangian characteristics of turbulence and scalar transport in direct numerical simulations. J. Fluid Mech. 427, 241–586.

Yeung, P.K., Pope, S.B., 1989. Lagrangian statistics from direct numerical simulations of isotropic turbulence. J. Fluid Mech. 207, 531–586.

Zaichik, L.I., 1997. Modelling of the motion of particles in non-uniform turbulent flow using the equation for the probability density function. Appl. Math. Mech. 61 (1), 127–133.

Zaichik, L.I., 1999. A statistical model of particle transport and heat transfer in turbulent shear flows. Phys. Fluids 11 (6), 1521–1534.

Zaichik, L.I., Alipchenkov, V.M., 2003. Pair dispersion and preferential concentration of particles in isotropic turbulence. Phys. Fluids 15 (6), 1776–1787.

Zaichik, L.I., Nigmatulin, B.I., Pershukov, V.A., 1995. Modelling of dynamics of aerosols in near-wall turbulent flows and particle deposition in pipes. In: Serizawa, A., Fukano, T., Batalle, J. (Eds.), Advancees in Multiphase Flow 1995. Elsevier, Amsterdam, pp. 75–84.

Zaichik, L.I., Vinberg, A.A., 1991. Modelling of particle dynamics and heat transfer in turbulent flows using equations for the first and second moments of velocity and temperature fluctuations. In: Proceedings of the Eighth Symposium on Turbulent Shear Flows, Munich, Germany, pp. 1021–1026.